doi:10.1093/jmcb/mjz085
Published online July 23, 2019

Review

Marking RNA: m^{6}A writers, readers, and functions in Arabidopsis

Marlene Reichel, Tino Köster, and Dorothee Staiger*

RNA Biology and Molecular Physiology, Faculty of Biology, Bielefeld University, 33615 Bielefeld, Germany
* Correspondence to: Dorothee Staiger, E-mail: dorothee.staiger@uni-bielefeld.de

Edited by Albrecht Bindereif

N^6-methyladenosine (m^{6}A) emerges as an important modification in eukaryotic mRNAs. m^{6}A has first been reported in 1974, and its functional significance in mammalian gene regulation and importance for proper development have been well established. An arsenal of writer, eraser, and reader proteins accomplish deposition, removal, and interpretation of the m^{6}A mark, resulting in dynamic function. This led to the concept of an epitranscriptome, the compendium of RNA species with chemical modification of the nucleobases in the cell, in analogy to the epigenome. While m^{6}A has long been known to also exist in plant mRNAs, proteins involved in m^{6}A metabolism have only recently been detected by mutant analysis, homology search, and mRNA interactome capture in the reference plant *Arabidopsis thaliana*. Dysregulation of the m^{6}A modification causes severe developmental abnormalities of leaves and roots and altered timing of reproductive development. Furthermore, m^{6}A modification affects viral infection. Here, we discuss recent progress in identifying m^{6}A sites transcriptome-wide, in identifying the molecular players involved in writing, removing, and reading the mark, and in assigning functions to this RNA modification in *A. thaliana*. We highlight similarities and differences to m^{6}A modification in mammals and provide an outlook on important questions that remain to be addressed.

Keywords: Arabidopsis, m^{6}A, mRNA interactome, posttranscriptional, RNA-binding protein

Introduction

Noncoding RNAs (ncRNAs) including ribosomal RNAs (rRNAs), transfer RNAs (tRNAs), spliceosomal small nuclear RNAs (snRNAs), and small nucleolar RNAs (snoRNAs) undergo extensive modification at the posttranscriptional level. Among more than hundred different nucleotide variants, methylation of adenosine at N^6 (m^{6}A) is a predominant type of internal covalent RNA modification (Fray and Simpson, 2015; Meyer and Jaffrey, 2017). In the early 1970s, m^{6}A modifications have been also found in mRNAs, both in mammals and plants. Nevertheless, they have only recently gained attention with respect to their function in regulating gene expression. The m^{6}A mark is deposited by dedicated proteins, the 'writers', is interpreted by 'readers', and can be removed by enzymatic activities, the 'erasers' (Meyer and Jaffrey, 2017; Balacco and Soller, 2019).

In higher plants, the detection of m^{6}A in the transcriptome of *Arabidopsis thaliana* and the prominent developmental abnormalities observed in mutants with altered m^{6}A levels has boosted the interest in this modification in the past few years. Exploiting the genetic resources and applying state-of-the-art high-throughput approaches in this model plant has led to novel insights into the m^{6}A methylome, to the identification of molecular players in m^{6}A metabolism (Table 1), and to insights into the function this modification plays in plant development and responses to environmental threats (Fray and Simpson, 2015; Burgess et al., 2016; Bhat et al., 2018; Kramer et al., 2018).

The m^{6}A methylome

An experimental hurdle for studying the m^{6}A distribution transcriptome-wide is the fact that it cannot be identified by conventional cDNA sequencing; in contrast to C to U or A to I conversions through RNA editing, adenosine methylation at the N^6 position still leads to T incorporation during reverse transcription, because the methyl group does not reside at the Watson–Crick base-pairing edge. Furthermore, the chemical features of adenosine and N^6-methylated adenosine are very similar, precluding chemical modification strategies to detect m^{6}A at single nucleotide resolution, as done, for example, for 5-methylcytosine (Squires et al., 2012). Rather, transcriptome-wide identification of m^{6}A sites has been possible through RNA immunoprecipitation using antibodies specific for m^{6}A, followed by RNA-seq of the co-precipitated RNAs, a method designated m^{6}A-seq (Dominissini et al., 2012) or m^{6}A-specific

Received January 17, 2019. Revised June 24, 2019. Accepted July 2, 2019.

Table 1 Orthologues of mammalian m^{6}A writers, readers, and erasers in *Arabidopsis thaliana*.

Arabidopsis	Orthologues in mammals	Phenotype of Arabidopsis loss-of-function mutants	References
Writer complex			
MTA	METTL3	Defective embryogenesis, abnormal flower morphology in hypomorphic adult plants	Vespa et al. (2004), Zhong et al. (2008), Bodi et al. (2012)
MTB	METTL14		Ruzicka et al. (2017)
FIP37	WTAP	Defective embryogenesis, overproliferation of stem cells in shoot apical meristem in hypomorphic adult plants	Zhong et al. (2008), Shen et al. (2016)
VIRILIZER	VIRMA/KIAA1429	Aberrant formation of lateral roots and root cap, aberrant development of cotyledons	Ruzicka et al. (2017)
HAKAI	HAKAI/Casitas B-lineage lymphoma-transforming sequence-like protein 1 (CBLL-1)/Cbl proto-oncogene like 1	Aphenotypic	Ruzicka et al. (2017)
Sequence not detected	Flacc/ZC3H13		Balacco and Soller (2019)
Readers			
ECT2	YTHDF1/2/3	Increased trichome branching, delayed leaf initiation	Arribas-Hernández et al. (2018), Scutenaire et al. (2018), Wei et al. (2018)
ECT3	YTHDF1/2/3	Increased trichome branching, delayed leaf initiation	Arribas-Hernández et al. (2018), Scutenaire et al. (2018), Wei et al. (2018)
ECT4	YTHDF1/2/3	Delayed leaf initiation	Arribas-Hernández et al. (2018)
Erasers			
atALKBH9B	AlkB5	Impaired AMV infection	Martinez-Perez et al. (2017)
atALKBH10B	AlkB5	Late flowering, reduced growth rate of leaves	Duan et al. (2017)
Sequence not detected	FTO		Balacco and Soller (2019)
N^6-mAMP deaminase			
*At*ADAL/MAPDA	*Hs*ADAL	Slight reduction in root growth	Chen et al. (2018)

methylated RNA immunoprecipitation (MeRIP)-seq (Meyer et al., 2012), respectively. m^{6}A sites are determined with a resolution of about 200 nucleotides. One m^{6}A peak was found about every 2000 nucleotides in mammals. Thus, if m^{6}A marks would be distributed equally, a transcript would have on average 1.7 peaks (Dominissini et al., 2012). This correlates well with early estimates of three m^{6}A marks per transcript obtained by determining the proportion of m^{6}A among all nucleotides in mouse cells (Perry et al., 1975).

More recently, a UV crosslinking step has been added to covalently bind the antibody to the m^{6}A mark. Similar to photoactivatable ribonucleoside-enhanced crosslinking and immunoprecipitation crosslinking (PAR-CLIP) detecting *in vivo* RNA–protein interaction sites genome-wide in human embryonic kidney 293 (HEK293) cells (Hafner et al., 2010), HeLa cells were fed with 4-thiouridine (4-SU) with the rationale that some 4-SU is incorporated close to m^{6}A sites (Chen et al., 2015). 4SU-containing mRNA is then purified by oligo (dT) capture and subjected to precipitation with the m^{6}A antibody before irradiation with 365 nm UV light in this photo crosslinking-assisted (PA)-m^{6}A-seq (Chen et al., 2015). After limited digestion of the crosslinked RNA and proteinase K digestion of the antibody, libraries are constructed. Because the crosslinked 4-SU is read as C during reverse transcription, resulting mutations are indicative of a close-by m^{6}A site, increasing the resolution to about 30 nucleotides compared to m^{6}A-seq and MeRIP-seq.

Another approach was to modify the HITS-CLIP technique that uses 254 nm UV light to crosslink RNA and bound proteins *in vivo* (Ule et al., 2003). In m^{6}A-CLIP, RNA is fragmented before incubation with the m^{6}A antibody. UV irradiation leads to crosslinking of the antibody at the m^{6}A site. After precipitation of the m^{6}A containing oligonucleotide and proteinase K digestion of the antibody, the residual peptide at the crosslink site leads to mutations or truncations during reverse transcription that are diagnostic for the modification site (Ke et al., 2015).

A similar approach employing m^{6}A precipitation and UV crosslinking subsequently generated the sequencing libraries according to the individual resolution nucleotide crosslinking and immunoprecipitation (iCLIP) protocol developed for mapping RNA–protein interactions transcriptome-wide with single nucleotide resolution in mammalian cells (König et al., 2010; Müller-McNicoll et al., 2016). Due to intramolecular circularization and relinearization of the cDNAs, the antibody-induced truncations at the m^{6}A site correspond to the nucleotide immediately upstream of the read. This approach is known as methyl iCLIP (miCLIP) (Linder et al., 2015).

These global studies in human and mouse cells showed that the m^{6}A distribution on mRNAs is highly selective, with a preference for the 3′ untranslated region 3′UTR, the coding sequence and the region around the stop codon (Dominissini et al., 2012; Meyer et al., 2012). Recent results suggest that increasing m^{6}A levels mark the early region of the last exon rather than the

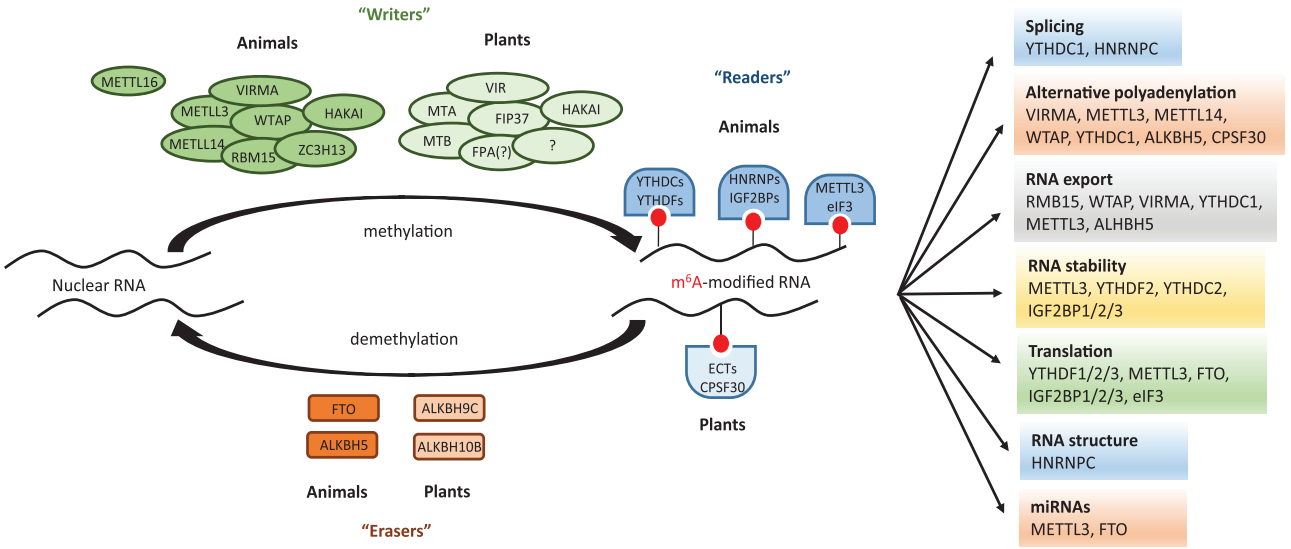

Figure 1 Schematic overview of the m⁶A machinery in plants and mammals. m⁶A is deposited on RNAs by 'writers', removed by 'erasers', and interpreted by 'readers'. m⁶A RNA methylation is involved in almost all steps of RNA metabolism including splicing, alternative polyadenylation, RNA export, RNA stability, translation, RNA structure, and miRNA regulation.

stop codon *per se* (Ke et al., 2015). In addition, m⁶A is found in ncRNAs and RNA viruses (Brocard et al., 2017). m⁶A sites are enriched in the previously established consensus sequence RRA*CH (R = G/A, H = A/C/U, * = methylation) (Wei and Moss, 1977; Harper et al., 1990; Dominissini et al., 2012).

An additional refinement of m⁶A probing aimed at determining the m⁶A methylome separately for three subcellular fractions, the chromatin-associated nascent pre-mRNAs, nucleoplasmic, and cytoplasmic mRNAs in HeLa cells (Ke et al., 2017). These data substantiated previous findings that m⁶A is mainly found in exons but rarely in introns, as chromatin-associated nascent RNA harbors many unspliced introns in contrast to poly(A) RNA usually employed for mapping of m⁶A. The m⁶A landscape in these fractions showed an overlap of ~90%, suggesting that the overall m⁶A patterns do not change much once the pre-mRNA is released from the chromatin into the nucleoplasm and following the export to the cytoplasm (Ke et al., 2017).

Importantly, the m⁶A methylome dynamically changes during development and in response to external stimuli. SCARLET (site-specific cleavage and radioactive-labeling followed by ligation-assisted extraction and thin-layer chromatography) allows determining the precise location and modification status of specific m⁶A sites. It has been estimated that the methylation status for a particular m⁶A site can vary between 6% and 80% and that many consensus motifs are not modified under particular conditions (Liu et al., 2013b).

In plants, m⁶A in mRNAs was first detected in maize (Nichols, 1979). Only much later was it also discovered in Arabidopsis poly(A) RNA using 2D thin-layer chromatography (Zhong et al., 2008; Bodi et al., 2012). It was found that m⁶A is not uniformly distributed along the RNAs but is enriched toward the end of the transcripts. More recently, m⁶A has been mapped transcriptome-wide in Arabidopsis using m⁶A-seq (Luo et al., 2014). Again, it is the most frequent internal modification of mRNAs, with 75% of transcripts harboring at least one m⁶A site. m⁶A sites were enriched around the stop codon and within 3′UTRs, as found in mammals. Additionally, m⁶A was enriched around the start codons in this study (Luo et al., 2014). Albeit, m⁶A sequencing of three different Arabidopsis organs, leaves, flowers, and roots found an enrichment predominantly near the stop codon and in the 3′UTR (Wan et al., 2015). Around 70% of the transcripts were modified by m⁶A with an average of 1.4 to 2 m⁶A sites per transcript. Above 75% of the fragments recovered by RNA immunoprecipitation (RIP) contained the consensus sequence RRA*CH described in mammals, with AAA*CU and AAA*CA being the most frequent motifs, consistent with previous findings (Luo et al., 2014). Most of the methylated mRNA displayed the typical topology found in Arabidopsis with one or two high peaks at the stop codon or in the 3′UTR and very low m⁶A signals in the coding regions (Wan et al., 2015).

A comparison among the three organs revealed that >80% of the m⁶A-modified transcripts were common between leaves, flowers, and roots. One third of the transcripts showed differential m⁶A methylation among the organs whereas only one fourth showed differences in steady-state levels. Moreover, transcripts with particularly high methylation in one organ encode unique functions for this organ, e.g. photosynthesis, carbohydrate, and nitrogen metabolism in leaves, RNA degradation pathways, DNA synthesis, and protein synthesis in flowers, as well as alkaloid biosynthesis and carbonate metabolism in roots (Wan et al., 2015). This suggests that m⁶A methylation makes an important contribution to organ differentiation.

A direct comparison of the m⁶A profile has been performed for two Arabidopsis ecotypes, Can-0 and Hen-16 (Luo et al., 2014). Despite a substantial conservation in the patterns between the ecotypes, a suite of the common m⁶A peaks showed ecotype-

specific changes in intensity in addition to peaks found exclusively in one of the ecotypes (Luo et al., 2014). In addition, m^{6}A was also identified in the genomes of alfalfa mosaic virus and cucumber mosaic virus (see below) (Martinez-Perez et al., 2017).

Writers

In mammals, a high molecular weight protein complex of ~1 MDa, the methylosome, is responsible for deposition of the m^{6}A mark (Figure 1; Bokar et al., 1994; Liu et al., 2013a). This complex comprises methyltransferase-like protein 3 (METTL3), the active adenosine methyltransferase that binds the cofactor S-adenosyl methionine (SAM) (Bokar et al., 1997). METTL3 interacts with methyltransferase-like 14 (METTL14). A crystal structure of the METTL3–METTL14 heterodimer loaded with SAM identified the residues D337, D395, N539, and E532 as being critical for the enzymatic activity of METTL3 (Wang et al., 2016). In metazoa, D395, N539, and E532 are not conserved in METTL14. This may correlate with the observation that human METTL14 does not methylate N^{6}A *in vitro* but may rather act to structurally support METTL3 (Wang et al., 2016; Schöller et al., 2018).

Additionally, the methylosome comprises a number of regulatory subunits. WILMS' TUMOR 1-ASSOCIATING PROTEIN (WTAP) stabilizes the interaction between METTL3 and METTL14 (Liu et al., 2013a; Ping et al., 2014; Schwartz et al., 2014). Moreover, it localizes METTL3 and METTL14 to nuclear speckles, which serve as a reservoir for splicing factors (Ping et al., 2014). Virilizer-like m^{6}A methyltransferase associated protein (VIRMA/KIAA1429), a mammalian homolog of Drosophila Virilizer involved in splicing of a sex-determination factor, was identified through its interaction with METTL3 (Schwartz et al., 2014). The VIRMA N-terminus binds to the WTAP–METTL3–METTL14 complex via WTAP in an RNA-independent manner in HeLa cells (Yue et al., 2018), but how VIRMA is required for m^{6}A methylation is unknown.

Similarly, RNA-binding motif protein 15 (RBM15) interacts with METTL3 dependent on WTAP in HEK293T cells (Patil et al., 2016). RBM15 belongs to the split end protein (Spen) family with three RNA-recognition motifs at the N-terminus and a Spen paralogues and orthologues C-terminal (SPOC) domain that engages in protein–protein interaction and has been suggested to function as an adapter protein recruiting the m^{6}A methylosome to specific regions within transcripts (Patil et al., 2016). Another auxiliary subunit is Fl(2)d-associated complex component (Flacc) in Drosophila, the counterpart of mammalian Zinc finger CCCH domain-containing protein 13 (ZC3H13), an animal-specific protein that bridges WTAP and RBM15 (Balacco and Soller, 2019; Knuckles et al., 2018).

In Arabidopsis, orthologues of several methylosome subunits have been identified and shown to interact with each other (Figure 1). Inactivation of METHYLTRANSFERASE A (MTA), the orthologue of METTL3, led to embryo-lethality and reduced m^{6}A levels in transcripts of the arrested seeds (Zhong et al., 2008). Complementation of the *mta* mutant by MTA driven by the seed-specific *ABSCISIC ACID INSENSITIVE 3* promoter allows overcoming the defect in embryo development. Reduced levels of MTA in the resulting hypomorphic adult plants lead to abnormal flower architecture and trichomes with a higher number of branches (Bodi et al., 2012).

MTA interacts *in vitro* and *in vivo* with *A. thaliana* FKBP12 INTERACTING PROTEIN 37 (FIP37), a homolog of WTAP (Zhong et al., 2008). Subsequently, WTAP was also found in the METTL3 complex in humans (Liu et al., 2013a; Ping et al., 2014). *Fip37-4* mutants have only 10% of the m^{6}A level and are embryo-lethal, similar to *mta* mutants. Again, complementation with FIP37 expressed from the embryo-specific *LEAFY COTYLEDON* promoter allowed to rescue adult plants (Shen et al., 2016). The very low *FIP37* expression in these plants led to massive proliferation of the stem cells in the shoot apical meristem that delivers aerial parts throughout the lifespan of the plant. This correlated with loss of m^{6}A marks in the mRNA for two stem cell regulators, *WUSCHEL* (*WUS*) and *SHOOT MERISTEMLESS* (*STM*), and an increase in the domain expressing *WUS*. Notably, the m^{6}A peak at the *WUS* and *STM* stop codons was reduced in *fip37-4 LEC1:FIP37*, correlating with reduced RNA degradation. RIP showed that FIP37 interacts with both *WUS* and *STM* transcripts in the shoot apex, pointing to a scenario where FIP37 *in vivo* binding promotes distinct m^{6}A modification with concomitant limitation of mRNA half-life. Elevated levels of FIP37 lead to a higher number of trichomes with supernumerary branches, similar to what was observed for mutants with reduced MTA levels (Vespa et al., 2004). This may indicate that the m^{6}A level needs to be precisely balanced, or alternatively, an excess of FIP37 has a dominant negative effect, perhaps interfering with methylosome assembly or function.

A screen for regulators of Arabidopsis vascular development identified a protein with homology to VIRMA/KIAA1429 involved in m^{6}A formation in mammals (Schwartz et al., 2014). In the Arabidopsis *vir-1* mutant, m^{6}A levels were reduced to ~10% and the mutant showed aberrant formation of lateral roots and root caps as well as aberrant cotyledon development (Ruzicka et al., 2017). A proteomics search for VIR-interacting proteins again identified FIP37 in cell suspension cultures. In addition, METHYLTRANSFERASE B (MTB) was recovered, which is an orthologue of human METTL14 (Ruzicka et al., 2017). As mentioned above, METTL14 lacks residues critical for enzymatic activity. Notably, these residues are conserved in Arabidopsis and other plants, suggesting that MTB may display enzymatic activity in some plants (Balacco and Soller, 2019). In an inducible MTB RNAi line m^{6}A levels were reduced to 50% (Ruzicka et al., 2017).

An additional component of the Arabidopsis writer complex was HAKAI, the orthologue of an E3 ubiquitin ligase (Ruzicka et al., 2017). Although m^{6}A levels are reduced to 35% in the *hakai* mutants, there are no obvious phenotypes. In mammals, Hakai interacts with WTAP, and knockdown in HeLa cells leads to reduction of m^{6}A levels by 23% (Yue et al., 2018). Flacc homologs have not been identified in Arabidopsis so far (Balacco and Soller, 2019). The Arabidopsis homolog of RBM15 is FPA, which regulates flowering time by RNA-mediated chromatin silencing of the floral repressor *FLOWERING LOCUS C* (*FLC*) (Bäurle et al., 2007). FPA controls *FLC* transcription by mediating

alternative polyadenylation of embedded noncoding antisense RNAs, which leads to downregulation of *FLC* transcription (Hornyik et al., 2010). However, a role of FPA in m^{6}A RNA methylation has not yet been demonstrated.

In mammals, apart from the METTL3–METTL14 writer complex, which is the major methyltransferase enzyme acting on polyadenylated mRNA, METTL16 can also methylate mRNA as well as U6 snRNA and various lncRNAs in humans (Warda et al., 2017; Pendleton et al., 2017). Interestingly, METTL16 is not a paralogue of METTL3 and METTL14 but part of a different methyltransferase protein family.

Readers

The m^{6}A mark is decoded by reader proteins to mediate the downstream effects on posttranscriptional regulation (Figure 1). Best understood are YTH (YT512-B homology) domain proteins, which were identified as m^{6}A-binding proteins in RNA-affinity chromatography using methylated RNA substrates as baits in mammals (Dominissini et al., 2012). The crystal structures of the human YTH domain revealed that three tryptophan residues, Trp411, Trp465, and Trp470, are crucial for m^{6}A binding, forming a buried hydrophobic aromatic cage where the 6-methylamino group is accommodated (Li et al., 2014; Luo and Tong, 2014; Theler et al., 2014; Xu et al., 2014; Zhu et al., 2014). This pocket is conserved in animals and plants and discriminates between m^{6}A and non-methylated mRNA with an increase in affinity of 20–50-fold. However, the YTH domain alone has low affinity for mRNA and needs additional low complexity protein regions, which assist in mRNA binding.

The YTH domain proteins are classified in two clades, the nuclear YTHDC proteins and YTHDF proteins that are mainly in the cytoplasm. Humans have two YTHDC proteins (YTHDC1 and YTHDC2) and three YTHDF proteins (YTHDF1, YTHDF2, and YTHDF3). YTHDC1 interacts with m^{6}A in nuclear RNA to regulate pre-mRNA splicing and polyadenylation (Xiao et al., 2016; Kasowitz et al., 2018), while YTHDF1, YTHDF2, and YTHDF3 interact with mature mRNAs in the cytoplasm to affect their stability. A systematic homology search unveiled that the Arabidopsis genome harbors 13 YTH domain proteins, which have arisen from multiple duplication events. Due to their conserved C-terminal region they were termed EVOLUTIONARILY CONSERVED C-TERMINAL REGION (ECT). ECT1–ECT11 belong to the DF clade and the other two belong to the DC clade (Arribas-Hernández et al., 2018; Scutenaire et al., 2018).

ECT proteins were initially associated with calcium signaling (Ok et al., 2005) and were only recently validated as RNA-binding proteins through mRNA interactome capture studies (Marondedze et al., 2016; Reichel et al., 2016; Köster et al., 2017). ECT2 binds m^{6}A-containing RNA *in vitro* and *in vivo*, and binding is abolished by mutation of tryptophane residues of the aromatic cage (Scutenaire et al., 2018; Wei et al., 2018). Mutants defective in ECT2 share a particular phenotype with mutants defective in writer proteins, namely increased branching of trichomes (Arribas-Hernández et al., 2018; Scutenaire et al., 2018; Wei et al., 2018). Trichome cells have undergone endoreduplication and thus have an increased DNA content, with the number of trichome branches directly correlating to ploidy levels (Vespa et al., 2004). In the *ect2* trichomes, the DNA content is elevated, indicating that the *ect2* trichomes underwent extra rounds of replication without cell division (Scutenaire et al., 2018). The trichome branching phenotype is complemented by wild-type ECT2 but not a mutated version with the three aromatic cage tryptophanes changed, indicating that ECT2 binding to m^{6}A underlies the phenotype (Arribas-Hernández et al., 2018). Mutants deficient in both, ECT2 and ECT3, also display a delayed leaf initiation rate from the shoot apical meristem (Arribas-Hernández et al., 2018).

Wei and colleagues developed a formaldehyde crosslinking and immunoprecipitation (FA-CLIP) strategy to identify ECT2-RNA interaction sites transcriptome-wide (Wei et al., 2018). They found 3680 transcripts with ECT2 binding sites that were strongly enriched in the 3′UTRs and identified a plant-specific ECT2 binding motif, URUAY. The motif was found 30 to 150 nucleotides upstream of poly(A) sites. In the *ect2* mutant, the majority of ECT2 binding targets were expressed at lower levels in contrast to non-targets. This has been taken as evidence that ECT2 promotes m^{6}A-dependent stability in contrast to mammalian YTHDF2 that promotes RNA degradation, albeit direct measurements of RNA stability for individual transcripts remain to be done. It should be kept in mind that formaldehyde leads not only to nucleic acid–protein crosslinks but also to protein–protein crosslinks; therefore, FA-CLIP is likely to also recover indirect targets.

A further YTH domain protein in Arabidopsis is CLEAVAGE AND POLYADENYLATION SPECIFICITY FACTOR 30 (AtCPSF30), which functions as part of a larger complex in mRNA 3′-end formation (Hunt et al., 2012). Analyses of *cpsf30* mutants indicated roles in oxidative stress responses (Zhang et al., 2008), plant immunity, and programmed cell death (Bruggeman et al., 2014), apart from altered mRNA 3′-end cleavage site choice (Thomas et al., 2012). Arabidopsis *CPSF30* gives rise to two protein variants through alternative polyadenylation: a shorter form of ~28 kDa that harbors three zinc finger domains and is homologous to yeast and mammalian CPSF30 and a longer form of ~70 kDa that additionally has a YTH domain and is unique to plants (Delaney et al., 2006; Hunt et al., 2012). Whether CPSF30 indeed interacts with m^{6}A and whether there is a link to 3′-end formation remains to be determined.

Apart from YTH domain proteins, other RNA binding proteins have been suggested to function as m^{6}A readers in mammals. METTL3, for instance, can act as an m^{6}A reader, independently of its function as a writer (Lin et al., 2016). It was shown to bind m^{6}A in the vicinity of the stop codon and engage in circularization of the mRNA through interaction with the eukaryotic initiation factor 3h (eIF3h), thus promoting translation (Choe et al., 2018).

Moreover, HNRNPA2B1 binds m^{6}A-bearing RNAs *in vivo* and *in vitro* and its biochemical footprint matches the m^{6}A consensus motif (Alarcón et al., 2015a). The K-homology domain containing insulin-like growth factor 2 mRNA-binding protein (IGF2BP) binds to thousands of mRNA transcripts through recognizing the consensus RRA*CH sequence and promotes their stability (Huang

et al., 2018). Recently, proline rich coiled-coil 2 A (Prrc2a) was identified as another reader that stabilizes a transcript involved in the specification of oligodendrocytes in an m^{6}A-dependent manner (Wu et al., 2019). The plethora of reader proteins without the dedicated binding cage suggests that additional proteins may be identified to interpret the m^{6}A mark, either directly or indirectly.

Erasers

Proteins implicated in removal of the m^{6}A methyl group belong to the family of AlkB homologous proteins comprising nonheme Fe (II) α-ketoglutarate-dependent dioxygenases (Figure 1; Jia et al., 2011; Zheng et al., 2013). In animals, the protein family includes fat mass and obesity-associated protein (FTO) and ALKBH5 that act as RNA m^{6}A demethylases. Overexpression or depletion of FTO led to subtle changes in m^{6}A (Jia et al., 2011). In the brain of knockout mice, adenosine methylation increased in some mRNAs important for neuronal signaling (Hess et al., 2013). FTO is also highly expressed in acute myeloid leukemia and inhibits normal hematopoiesis by decreasing m^{6}A levels in specific transcripts, leading to their reduced stability (Li et al., 2017b). Recently, it has been shown that FTO also demethylates m^{6}A$_m$, the first nucleotide of the 5′ cap (Mauer et al., 2017). FTO exhibits nearly 100 times greater catalytic activity against m^{6}A$_m$ compared to m^{6}A, leading to the speculation that FTO mostly acts on m^{6}A$_m$ and only on a few specific m^{6}A sites. Apart from the controversy about the physiological target of FTO, concerns have also been raised about the reversibility of m^{6}A methylation in general, since Darnell and colleagues showed that m^{6}A is retained in mRNA exons until the mRNA is degraded (Darnell et al., 2018). FTO is conserved among eukaryotes but absent in Arabidopsis (Balacco and Soller, 2019).

In the Arabidopsis genome, 13 ALKHB family proteins are predicted with diverse subcellular localization (Mielecki et al., 2012). Of five proteins with homology to ALKBH5 (Duan et al., 2017), atALKBH9B demethylates m^{6}A in single-stranded RNA *in vitro* (Martinez-Perez et al., 2017). As mentioned above, m^{6}A marks were found in plant RNA viruses. In *atalkbh9b* mutants, the genomic alfalfa mosaic virus RNAs show increased levels of m^{6}A. This correlates with impaired accumulation of the virus and reduced spreading in infected Arabidopsis plants, suggesting that atALKBH9B demethylates m^{6}A *in vivo* (Martinez-Perez et al., 2017).

In contrast, Duan et al. (2017) did not observe changes in the m^{6}A/A ratio in *atalkbh9b* and *atalkbh9c* mutants. Rather, atALKBH10B was shown to demethylate m^{6}A marks *in vitro* and *in vivo*, and *atalkbh10b* mutants had increased m^{6}A levels (Duan et al., 2017). Overexpression of atALKBH10B leads to early flowering whereas *atalkbh10b* mutants flower later than wild-type plants. The delayed transition to reproductive development was corrected by wild-type atALKBH10B but not by a catalytically dead variant, atALKBH10B$^{H366A/E368A}$. In the mutant, the floral integrator *FLOWERING LOCUS T* (*FT*) and two transcriptional activators of *FT* expression, *SQUAMOSA PROMOTER BINDING PROTEIN-LIKE 3* (*SPL3*) and *SPL9* mRNA showed reduced levels (Duan et al., 2017). This correlated with higher m^{6}A levels around the *FT* start and stop codons and within the *SPL3* and *SPL9* 3′UTRs and faster degradation in the mutant. Direct *in vivo* binding of atALKBH10B to *FT*, *SPL3,* and *SPL9* indicates that atALKBH10B demethylates floral activators to control their half-life and consequently, accumulation. Thus, m^{6}A emerges as yet another factor to be added to the regulatory network of floral transition (Srikanth and Schmid, 2011; Johansson and Staiger, 2015).

Impact of m^{6}A on RNA processing steps

Alternative splicing

Early on, m^{6}A has been linked to splicing, as changes in alternative splicing have been observed upon knockdown of METTL3, FTO, or ALK5B (Ping et al., 2014; Bartosovic et al., 2017; Tang et al., 2018). However, the number of targets affected varied widely in different cells studied (Martinez and Gilbert, 2018). Recently, transient N^6 methyladenosine transcriptome sequencing (TNT-seq) on BrdU labeled nascent RNA and quantitative TNT pulse-chase sequencing were developed to assess the impact of m^{6}A on splicing kinetics with high temporal resolution in HEK293 cells (Louloupi et al., 2018). These experiments showed that a significant fraction of m^{6}A sites are deposited early near splice site junctions in exons and promote fast splicing, whereas m^{6}A sites in introns are associated with slower splicing kinetics and alternative splicing (Louloupi et al., 2018).

The effect of m^{6}A on alternative splicing can be mediated by YTHDC1, which interacts with the splicing factor SRSF3 to increase its ability to bind RNA and promotes exon inclusion. In contrast, YTHDC1 and SRSF3 block RNA binding of SRSF10, a factor that stimulates exon exclusion (Xiao et al., 2016). Furthermore, METTL16 promotes the expression of human MAT2A encoding SAM synthetase when SAM levels are low by enhanced splicing of a retained intron, resulting from binding to its target site in the MAT2A 3′UTR (Pendleton et al., 2017).

On the other hand, it was suggested that m^{6}A is not prominently required for splicing regulation. Comparing the m^{6}A methylome separately for three subcellular fractions, the chromatin-associated nascent pre-mRNAs, nucleoplasmic pre-mRNAs, and cytoplasmic mRNAs in HeLa cells revealed that only ∼10% of m^{6}As in chromatin-associated nascent pre-mRNAs are within 50 nucleotides of 5′ or 3′ splice sites. Furthermore, the vast majority of exons harboring m^{6}A in wild-type mouse stem cells is spliced the same in cells lacking METTL3 (Ke et al., 2017). Clearly, changes in overall m^{6}A levels can also have indirect effects on splicing. A dedicated role of an m^{6}A site in alternative splicing can be inferred from the analysis of splicing reporters with varying methylation levels of a defined site.

In Arabidopsis, a connection between m^{6}A and splicing has not yet been investigated. In *vir-1* mutants defective in the homolog of the Drosophila splicing factor VIR, no prominent changes in alternative splicing were detected (Ruzicka et al., 2017).

Alternative polyadenylation

The enrichment of m^{6}A sites at the beginning of the last exon and 3′UTR indicated an involvement in the choice of polyadeny-

lation sites (Ke et al., 2015). VIRMA provides a link between the writer complex and the polyadenylation machinery by recruiting the catalytic core components METTL3/METTL14/WTAP to the 3′UTR and interacting with the polyadenylation cleavage factors CPSF5 and CPSF6 (Yue et al., 2018). Of more than 2800 transcripts having their 3′UTR shortened upon CPSF5 knockdown, 84% have increased m^{6}A peak density in the 3′UTR and near the stop codon.

YTHDC1 also interacts with CPSF6, and loss of YTHDC1 in mouse oocytes influences alternative polyadenylation apart from the effect on splicing (Kasowitz et al., 2018). In mouse male germ cells, knockout of the eraser protein ALKBH5 also results in aberrant splicing and in the production of longer 3′UTRs (Tang et al., 2018).

In Arabidopsis, one of the two CPSF30 protein variants harbors a YTH domain and is involved in processing of 3′-ends, which are enriched in m^{6}A marks. Therefore, a role of m^{6}A in governing 3′-end formation has been also been proposed for plants (Chakrabarti and Hunt, 2015; Fray and Simpson, 2015; Burgess et al., 2016), but not yet experimentally validated.

mRNA export

Several reader and writer proteins have been connected to mRNA export by the TREX:NXF1 pathway (Lesbirel et al., 2018). Once an mRNA has matured, TREX recruits the export receptor NXF1, which guides the mRNA through the nuclear pore to the cytoplasm. It was shown that the m^{6}A writer complex associates with the TREX complex, and simultaneous knockdown of WTAP and VIRMA blocked export of a specific group of methylated transcripts (Lesbirel et al., 2018).

Interestingly, knockdown of RBM15 leads to cytoplasmic depletion and nuclear accumulation of mRNA (Uranishi et al., 2009; Zolotukhin et al., 2009). As RBM15 binds to NXF1, it may act as an export co-adaptor aiding in NXF1 loading on the mRNA. Furthermore, knockdown of METTL3 negatively affects the nuclear export of specific transcripts of circadian clock genes, resulting in long period circadian rhythms (Fustin et al., 2013).

Moreover, YTHDC1 was shown to interact with the splicing factor and nuclear export adaptor protein SRSF3, facilitating RNA binding to both SRSF3 and NXF1 (Roundtree et al., 2017). Knockdown of YTHDC1 or SRSF3 blocked nuclear export of a common set of transcripts suggesting the two proteins act in the same pathway. Thus, YTHDC1 was proposed to selectively mediate the export of m^{6}A-containing mRNAs (Roundtree et al., 2017). Additionally, ALKBH5-deficient mice show increased levels of m^{6}A containing transcripts in the nucleus leading to impaired fertility (Zheng et al., 2013).

mRNA stability

In mouse embryonic stem cells, knockdown of METTL3 and METTL14 and the resulting lack of m^{6}A RNA methylation led to a loss of self-renewal capability. For many transcripts, including transcripts encoding developmental regulators, m^{6}A methylation was inversely correlated with mRNA stability and gene expression (Wang et al., 2014b). Another study in HeLa and mouse embryonic stem cells also found that, upon knockout of METTL3, the half-lives of thousands of mRNAs increased at least 2-fold, indicating that mRNAs harboring m^{6}As have shorter half-lives (Ke et al., 2017).

Accordingly, YTHDF2 destabilizes m^{6}A-containing RNA by interacting with the CCR4-NOT complex in processing (P) bodies, which leads to poly(A) tail shortening and consequently to mRNA degradation (Wang et al., 2014a; Du et al., 2016). In addition, YTHDC2 acts as an adaptor recruiting the cytoplasmic 5′−3′ exonuclease Xrn1 via its ankyrin repeats on mRNA, promoting rapid degradation (Wojtas et al., 2017; Kretschmer et al., 2018). The YTHDC2 helicase activity is also essential for the decay of specific mitotic mRNAs for meiosis progression in mammalian germlines (Wojtas et al., 2017; Jain et al., 2018).

Recent evidence shows that m^{6}A may also increase mRNA stability. As described above, FTO overexpression in acute myeloid leukemia decreases the stability of specific transcripts upon a decrease in m^{6}A levels (Li et al., 2017b). Moreover, in contrast to the destabilizing function of YTHDF2, IGF2BP binding to mRNAs in an m^{6}A-dependent manner promotes their stability (Huang et al., 2018).

So far, stabilizing effects have been reported for the m^{6}A mark in Arabidopsis. Many m^{6}A-modified mRNAs in Arabidopsis have reduced abundance in the absence of this mark. The decrease in abundance is due to transcript destabilization caused by cleavage occurring 4 or 5 nucleotides directly upstream of unmodified m^{6}A sites (Anderson et al., 2018). Furthermore, ECT2 has been proposed to promote m^{6}A-dependent stability of binding targets (Wei et al., 2018). In contrast, the analysis of *fip37* mutants indicated that m^{6}A levels are inversely correlated with RNA levels in *WUS* and *STM* in the shoot apical meristem (Shen et al., 2016). Similarly, in the *atalkbh10b* mutant higher m^{6}A levels in *FT* and its regulators *SPL3* and *SPL9* correlate with faster degradation (Duan et al., 2017).

Translation

YTH domain proteins also play important roles in regulating translation. In the 5′UTR, m^{6}A can be bound by the translation factor eIF3 to recruit the 43S pre-initiation complex internally and initiate cap-independent translation (Meyer et al., 2015). In contrast, m^{6}A located near stop codons or in the 3′UTR is recognized by YTHDF1, which then interacts with eIF3 and other ribosome-associated proteins to stimulate cap-dependent ribosome loading (Wang et al., 2015). YTHDF3 interacts with YTHDF1 and has a synergistic effect on promoting translation by recruiting ribosomal proteins (Li et al., 2017a; Shi et al., 2017). METTL3 in the 3′UTR was also shown to interact with eIF3h bound to the translation start site to promote closed-loop conformation, stimulating translation through enhanced ribosome recycling (Lin et al., 2016; Choe et al., 2018).

m^{6}A is also involved in translational control in response to heat shock. Upon heat stress, YTHDF2 relocates to the nucleus where it binds to m^{6}A sites in the 5′UTR of stress-induced transcripts including HSP70, thereby preventing FTO from demethylation and promoting translation (Zhou et al., 2015). One study also

reported relocation of Arabidopsis ECT2 to stress granules upon heat stress, suggesting that m^{6}A might also play a role in plant stress response (Scutenaire et al., 2018).

In mammals, m^{6}A can also have a negative effect on translation, as FTO promotes translation of mRNAs involved in neural development (Yu et al., 2018). Together, these findings suggest that m^{6}A can affect translation via multiple mechanisms depending on cell type, developmental stage and cellular context.

m^{6}A effects on RNA structure

As mentioned above, methylation of N^6 does not affect the base pairing properties of adenine. Instead, m^{6}A leads to reduced stability of RNA duplexes and thus altered RNA secondary structure (Kierzek and Kierzek, 2003). m^{6}A in unpaired loop positions base-stacks stronger than the unmodified base, stabilizing the single-stranded regions (Roost et al., 2015). To determine the impact of m^{6}A on RNA secondary structure globally, Roost and coworkers intersected data on *in vivo* RNA secondary structure determined for a human cell line with m^{6}A peaks obtained by Me-RIP-seq. This revealed a tendency to single-stranded structure of the nucleotides adjacent to the m^{6}A (Roost et al., 2015). Thus, in addition to direct interpretation of m^{6}A by dedicated reader proteins, m^{6}A can affect the accessibility for RNA-binding proteins indirectly by altering RNA secondary structure (Liu et al., 2015; Liu et al., 2017).

m^{6}A in microRNAs

In mammals, METTL3 methylates pri-miRNAs to mark them for recognition by DGCR8 of the microprocessor complex. This modification promotes pri-miRNA processing (Alarcón et al., 2015b; Knuckles et al., 2017; Michlewski and Caceres, 2019). Human HNRNPA2B1 binds to the m^{6}A mark in a subset of pri-miRNAs and interacts with DGCR8, which then recruits DROSHA for processing (Alarcón et al., 2015a). While a suite of RNA-binding proteins including hnRNP-like proteins have also been shown to affect pri-miRNA processing in Arabidopsis at the post-transcriptional level, it is not known whether this involves m^{6}A (Dong et al., 2008; Ren et al., 2012; Ben Chaabane et al., 2013; Köster et al., 2014).

Demethylation also affects miRNA expression, as knockdown of FTO leads to aberrant miRNA steady-state levels (Berulava et al., 2015). m^{6}A marks within 3′UTRs have been generally associated with the presence of miRNA binding sites, where about 2/3 of mRNAs containing an m^{6}A site within their 3′UTR also have at least one miRNA binding site (Meyer et al., 2012; Chen et al., 2015)

Interestingly, miRNAs themselves positively regulate m^{6}A deposition on mRNAs via a sequence-pairing mechanism (Chen et al., 2015). Manipulation of miRNA expression or sequences alters m^{6}A levels through modulating binding of METTL3 to mRNAs containing miRNA targeting sites. In Arabidopsis, only ~1% of the 1000 most significant m^{6}A peaks are in regions potentially targeted by miRNAs, suggesting that m^{6}A is less likely to directly affect miRNA binding sites (Luo et al., 2014).

m^{6}A in ncRNAs

In addition to mRNAs, m^{6}A also occurs in a range of ncRNAs including U6 snRNA and lncRNAs. For instance, the lncRNA X-inactive specific transcript (XIST), which mediates silencing of the X-chromosome during female development in mammals, contains high levels of m^{6}A (Patil et al., 2016). YTHDC1 recognizes m^{6}A residues on XIST and is required for XIST function, while knockdown of RBM15 or METTL13 impairs X-mediated inactivation, indicating that m^{6}A is required for XIST function (Patil et al., 2016). XIST was also found to interact with METLL16 (Warda et al., 2017), but the function of this interaction is still unknown. METLL16 also binds to the 3′-region of the cancer-associated ncRNA metastasis-associated lung adenocarcinoma transcript 1 (MALAT-1). The presence of m^{6}A in MALAT-1 has been shown to alter RNA structure to facilitate binding of HNRNPC, a pre-mRNA processing protein (Liu et al., 2015).

In Arabidopsis, m^{6}A marks have also been found on ~10% of tRNAs, all rRNAs, and many snRNAs and snoRNAs (Wan et al., 2015; Shen et al., 2016), but the function remains to be determined.

Catabolism of m^{6}A degradation products

Although the methyl group of m^{6}A can be removed by erasers, m^{6}A levels also decrease due to RNA decay. Until recently, the fate of the resulting N^6 methylated AMP (N^6-mAMP) has remained enigmatic. Witte and co-workers now demonstrated the presence of an N^6-mAMP deaminase in Arabidopsis (Chen et al., 2018). Removal of the N^6-mAMP methyl group yields IMP. Because RNA polymerases are able to act on N^6-mAMP, this demethylation step may prevent mis-incorporation of modified adenosine into nascent transcripts. Subsequently, N^6-mAMP deaminase activity was also found in HeLa cells. Furthermore, the authors demonstrated that adenylate kinase strongly prefers AMP over N^6-mAMP, providing another safeguard mechanism against untargeted incorporation of m^{6}A (Chen et al., 2018).

Conclusions

Almost half a century after their first mention, m^{6}A modifications in mRNAs have moved center stage in plant RNA biology. Significant progress has been made to describe m^{6}A sites transcriptome-wide and identify the molecular players involved in installing, erasing, and interpreting the marks. Nevertheless, we only begin to appreciate the distribution of m^{6}A marks in the transcriptome, the proteins involved in m^{6}A metabolism, and the spectrum of processes affected by m^{6}A in plants. The similar m^{6}A consensus motifs in mammals and plants suggest that m^{6}A methylation may be conserved but also distinct differences were found.

So far, the m^{6}A methylome has been determined by m^{6}A-seq in Arabidopsis (Luo et al., 2014; Wan et al., 2015; Shen et al., 2016). In mammals, the inherent limitation to resolve m^{6}A peaks with a resolution of about 200 nucleotides has been overcome by incorporating a UV fixation step (Chen et al., 2015; Ke et al., 2015; Linder et al., 2015). In plants, UV irradiation

has been successfully employed in Arabidopsis to crosslink RNA and protein *in vivo* despite previous reservations about the efficiency of UV crosslinking in the presence of UV absorbing pigments in plant tissues, (Zhang et al., 2015; Reichel et al., 2016; Meyer et al., 2017). Thus, it should be feasible to increase the resolution of m^{6}A profiling also in plants. Moreover, the comparison between different reports is hampered by the fact that different facets of a protocol are applied, that the determination of m^{6}A peaks is accomplished by different bioinformatics pipelines, and that the quality of the antibody can be quite variable (Schwartz et al., 2013; Linder et al., 2015). Overall, how the methylosome achieves selectivity for specific transcripts and defined sites within the transcripts remains to be clarified.

Initial experiments point to extensive remodeling of the m^{6}A methylome during plant development and in response to stress (Wan et al., 2015; Anderson et al., 2018). To fully appreciate the regulatory potential, temporal and spatial changes have to be determined systematically across tissues and in response to abiotic and biotic factors which have a prominent effect on plants as sessile organisms.

Furthermore, there is a gap in understanding the molecular consequences of m^{6}A modification on mRNA processing and function, e.g. how processing factors are recruited. The impact of m^{6}A depends on the timing of deposition in the cell (Martinez and Gilbert, 2018). METTL3 associates with RNA polymerase II, linking the addition of the m^{6}A mark to transcription (Slobodin et al., 2017). Deposition in nascent RNA can affect all downstream processing steps including RNA stability in the cytoplasm. A first investigation of the m^{6}A landscape in separate chromatin-associated, nucleoplasmic and cytoplasmic fractions in HeLa cells showed an overlap of ~90% (Ke et al., 2017). However, methylation levels of distinct sites are likely to vary.

Whereas mammals have 5 YTF domain proteins, Arabidopsis harbors 13, raising the question about their function. For example, mutations of the close ECT2 homolog ECT4 enhanced the phenotype of *ect2 ect3* (Arribas-Hernández et al., 2018). A detailed characterization of their divergent expression patterns and a description of phenotypes of higher order mutants will unveil possible specific and redundant functions of all ECTs. Although the m^{6}A machinery is increasingly well characterized, novel proteins are still being discovered in mammals, such as the novel reader protein Prrc2a (Wu et al., 2019). This indicates that additional proteins may emerge as writers, readers, and erasers of the m^{6}A mark in Arabidopsis. Of note, a plethora of proteins with the capability of binding RNA have been identified in three recent mRNA interactome capture experiments, many of which have not yet been assigned a function in RNA metabolism (Marondedze et al., 2016; Reichel et al., 2016; Zhang et al., 2016; Köster et al., 2017).

Acknowledgements

The authors thank Dr Arribas-Hernandez for comments on an earlier draft of the manuscript.

Funding

Our research is funded by the German Research Foundation (grants STA653/9-1; STA/13-1 to D.S., KO5634/1-1 to T.K.) as well as by the Young Investigator Fund of Bielefeld University (M.R.).

Conflict of interest: none declared.

References

Alarcón, C.R., Goodarzi, H., Lee, H., et al. (2015a). HNRNPA2B1 is a mediator of m^{6}A-dependent nuclear RNA processing events. Cell *162*, 1299–1308.

Alarcón, C.R., Lee, H., Goodarzi, H., et al. (2015b). N^6-methyladenosine marks primary microRNAs for processing. Nature *519*, 482–485.

Anderson, S.J., Kramer, M.C., Gosai, S.J., et al. (2018). N^6-methyladenosine inhibits local ribonucleolytic cleavage to stabilize mRNAs in Arabidopsis. Cell Rep. *25*, 1146–1157.

Arribas-Hernández, L., Bressendorff, S., Hansen, M.H., et al. (2018). An m^{6}A-YTH module controls developmental timing and morphogenesis in Arabidopsis. Plant Cell *30*, 952–967.

Balacco, D.L., and Soller, M. (2019). The m^{6}A writer: rise of a machine for growing tasks. Biochemistry *58*, 363–378.

Bartosovic, M., Molares, H.C., Gregorova, P., et al. (2017). N^6-methyladenosine demethylase FTO targets pre-mRNAs and regulates alternative splicing and 3′-end processing. Nucleic Acids Res. *45*, 11356–11370.

Bäurle, I., Smith, L., Baulcombe, D.C., et al. (2007). Widespread role for the flowering-time regulators FCA and FPA in RNA-mediated chromatin silencing. Science *318*, 109–112.

Ben Chaabane, S., Liu, R., Chinnusamy, V., et al. (2013). STA1, an Arabidopsis pre-mRNA processing factor 6 homolog, is a new player involved in miRNA biogenesis. Nucleic Acids Res. *41*, 1984–1997.

Berulava, T., Rahmann, S., Rademacher, K., et al. (2015). N^6-adenosine methylation in miRNAs. PLoS One *10*, e0118438.

Bhat, S., Bielewicz, D., Jarmolowski, A., et al. (2018). N^6-methyladenosine (m^{6}A): revisiting the old with focus on new, an Arabidopsis thaliana centered review. Gene *9*, 596.

Bodi, Z., Zhong, S., Mehra, S., et al. (2012). Adenosine methylation in Arabidopsis mRNA is associated with the 3′ end and reduced levels cause developmental defects. Front. Plant Sci. *3*, 48.

Bokar, J.A., Rath-Shambaugh, M.E., Ludwiczak, R., et al. (1994). Characterization and partial purification of mRNA N^6-adenosine methyltransferase from HeLa cell nuclei. Internal mRNA methylation requires a multisubunit complex. J. Biol. Chem. *269*, 17697–17704.

Bokar, J.A., Shambaugh, M.E., Polayes, D., et al. (1997). Purification and cDNA cloning of the AdoMet-binding subunit of the human mRNA (N^6-adenosine)-methyltransferase. RNA *3*, 1233–1247.

Brocard, M., Ruggieri, A., and Locker, N. (2017). m^{6}A RNA methylation, a new hallmark in virus–host interactions. J. Gen. Virol. *98*, 2207–2214.

Bruggeman, Q., Garmier, M., de Bont, L., et al. (2014). The polyadenylation factor subunit CLEAVAGE AND POLYADENYLATION SPECIFICITY FACTOR 30: a key factor of programmed cell death and a regulator of immunity in Arabidopsis. Plant Physiol. *165*, 732–746.

Burgess, A., David, R., and Searle, I.R. (2016). Deciphering the epitranscriptome: a green perspective. J. Integr. Plant Biol. *58*, 822–835.

Chakrabarti, M., and Hunt, A.G. (2015). CPSF30 at the interface of alternative polyadenylation and cellular signaling in plants. Biomolecules *5*, 1151–1168.

Chen, K., Lu, Z., Wang, X., et al. (2015). High-resolution N^6-methyladenosine (m^{6}A) map using photo-crosslinking-assisted m^{6}A sequencing. Angew. Chem. Int. Ed. Engl. *54*, 1587–1590.

Chen, M., Urs, M.J., Sánchez-González, I., et al. (2018). m^{6}A RNA degradation products are catabolized by an evolutionarily conserved N^6-methyl-AMP deaminase in plant and mammalian cells. Plant Cell *30*, 1511–1522.

Choe, J., Lin, S., Zhang, W., et al. (2018). mRNA circularization by METTL3–eIF3h enhances translation and promotes oncogenesis. Nature *561*, 556–560.

Darnell, R.B., Ke, S., and Darnell, J.E., Jr. (2018). Pre-mRNA processing includes N^6 methylation of adenosine residues that are retained in mRNA exons and the fallacy of 'RNA epigenetics'. RNA *24*, 262–267.

Delaney, K., Xu, R., Li, Q.Q., et al. (2006). Calmodulin interacts with and regulates the RNA-binding activity of an Arabidopsis polyadenylation factor subunit. Plant Physiol. *140*, 1507–1521.

Dominissini, D., Moshitch-Moshkovitz, S., Schwartz, S., et al. (2012). Topology of the human and mouse m^6A RNA methylomes revealed by m^6A-seq. Nature *485*, 201–206.

Dong, Z., Han, M.H., and Fedoroff, N. (2008). The RNA-binding proteins HYL1 and SE promote accurate in vitro processing of pri-miRNA by DCL1. Proc. Natl Acad. Sci. USA *105*, 9970–9975.

Du, H., Zhao, Y., He, J., et al. (2016). YTHDF2 destabilizes m^6A-containing RNA through direct recruitment of the CCR4-NOT deadenylase complex. Nat. Commun. *7*, 12626.

Duan, H.-C., Wei, L.-H., Zhang, C., et al. (2017). ALKBH10B is an RNA N^6-methyladenosine demethylase affecting Arabidopsis floral transition. Plant Cell *29*, 2995–3011.

Fray, R.G., and Simpson, G.G. (2015). The Arabidopsis epitranscriptome. Curr. Opin. Plant Biol. *27*, 17–21.

Fustin, J.-M., Doi, M., Yamaguchi, Y., et al. (2013). RNA-methylation-dependent RNA processing controls the speed of the circadian clock. Cell *155*, 793–806.

Hafner, M., Landthaler, M., Burger, L., et al. (2010). Transcriptome-wide identification of RNA-binding protein and microRNA target sites by PAR-CLIP. Cell *141*, 129–141.

Harper, J.E., Miceli, S.M., Roberts, R.J., et al. (1990). Sequence specificity of the human mRNA N^6-adenosine methylase in vitro. Nucleic Acids Res. *18*, 5735–5741.

Hess, M.E., Hess, S., Meyer, K.D., et al. (2013). The fat mass and obesity associated gene (Fto) regulates activity of the dopaminergic midbrain circuitry. Nat. Neurosci. *16*, 1042–1048.

Hornyik, C., Terzi, L.C., and Simpson, G.G. (2010). The Spen family protein FPA controls alternative cleavage and polyadenylation of RNA. Dev. Cell *18*, 203–213.

Huang, H., Weng, H., Sun, W., et al. (2018). Recognition of RNA N^6-methyladenosine by IGF2BP proteins enhances mRNA stability and translation. Nat. Cell Biol. *20*, 285–295.

Hunt, A.G., Xing, D., and Li, Q.Q. (2012). Plant polyadenylation factors: conservation and variety in the polyadenylation complex in plants. BMC Genomics *13*, 641.

Jain, D., Puno, M.R., Meydan, C., et al. (2018). Ketu mutant mice uncover an essential meiotic function for the ancient RNA helicase YTHDC2. eLife *7*, e30919.

Jia, G., Fu, Y., Zhao, X., et al. (2011). N^6-methyladenosine in nuclear RNA is a major substrate of the obesity-associated FTO. Nat. Chem. Biol. *7*, 885–887.

Johansson, M., and Staiger, D. (2015). Time to flower: interplay between photoperiod and the circadian clock. J. Exp. Bot. *66*, 719–730.

Kasowitz, S.D., Ma, J., Anderson, S.J., et al. (2018). Nuclear m^6A reader YTHDC1 regulates alternative polyadenylation and splicing during mouse oocyte development. PLoS Genet. *14*, e1007412.

Ke, S., Alemu, E.A., Mertens, C., et al. (2015). A majority of m^6A residues are in the last exons, allowing the potential for 3′ UTR regulation. Genes Dev. *29*, 2037–2053.

Ke, S., Pandya-Jones, A., Saito, Y., et al. (2017). m^6A mRNA modifications are deposited in nascent pre-mRNA and are not required for splicing but do specify cytoplasmic turnover. Genes Dev. *31*, 990–1006.

Kierzek, E., and Kierzek, R. (2003). The thermodynamic stability of RNA duplexes and hairpins containing N^6-alkyladenosines and 2-methylthio-N^6-alkyladenosines. Nucleic Acids Res. *31*, 4472–4480.

Knuckles, P., Carl, S.H., Musheev, M., et al. (2017). RNA fate determination through cotranscriptional adenosine methylation and microprocessor binding. Nat. Struct. Mol. Biol. *24*, 561–569.

Knuckles, P., Lence, T., Haussmann, I.U., et al. (2018). Zc3h13/Flacc is required for adenosine methylation by bridging the mRNA-binding factor Rbm15/Spenito to the m^6A machinery component Wtap/Fl(2)d. Genes Dev. *32*, 415–429.

König, J., Zarnack, K., Rot, G., et al. (2010). iCLIP reveals the function of hnRNP particles in splicing at individual nucleotide resolution. Nat. Struct. Mol. Biol. *17*, 909–915.

Köster, T., Marondedze, C., Meyer, K., et al. (2017). RNA-binding proteins revisited—the emerging Arabidopsis mRNA interactome. Trends Plant Sci. *22*, 512–526.

Köster, T., Meyer, K., Weinholdt, C., et al. (2014). Regulation of pri-miRNA processing by the hnRNP-like protein AtGRP7 in Arabidopsis. Nucleic Acids Res. *42*, 9925–9936.

Kramer, M.C., Anderson, S.J., and Gregory, B.D. (2018). The nucleotides they are a-changin': function of RNA binding proteins in post-transcriptional messenger RNA editing and modification in Arabidopsis. Curr. Opin. Plant Biol. *45*, 88–95.

Kretschmer, J., Rao, H., Hackert, P., et al. (2018). The m^6A reader protein YTHDC2 interacts with the small ribosomal subunit and the 5′–3′ exoribonuclease XRN1. RNA *24*, 1339–1350.

Lesbirel, S., Viphakone, N., Parker, M., et al. (2018). The m^6A-methylase complex recruits TREX and regulates mRNA export. Sci. Rep. *8*, 13827.

Li, A., Chen, Y.-S., Ping, X.-L., et al. (2017a). Cytoplasmic m^6A reader YTHDF3 promotes mRNA translation. Cell Res. *27*, 444–447.

Li, F., Zhao, D., Wu, J., et al. (2014). Structure of the YTH domain of human YTHDF2 in complex with an m^6A mononucleotide reveals an aromatic cage for m^6A recognition. Cell Res. *24*, 1490–1492.

Li, Z., Weng, H., Su, R., et al. (2017b). FTO plays an oncogenic role in acute myeloid leukemia as a N^6-methyladenosine RNA demethylase. Cancer Cell *31*, 127–141.

Lin, S., Choe, J., Du, P., et al. (2016). The m^6A methyltransferase METTL3 promotes translation in human cancer cells. Mol. Cell *62*, 335–345.

Linder, B., Grozhik, A.V., Olarerin-George, A.O., et al. (2015). Single-nucleotide-resolution mapping of m^6A and m^6Am throughout the transcriptome. Nat. Methods *12*, 767.

Liu, J., Yue, Y., Han, D., et al. (2013a). A METTL3–METTL14 complex mediates mammalian nuclear RNA N^6-adenosine methylation. Nat. Chem. Biol. *10*, 93.

Liu, N., Dai, Q., Zheng, G., et al. (2015). N^6-methyladenosine-dependent RNA structural switches regulate RNA–protein interactions. Nature *518*, 560.

Liu, N., Parisien, M., Dai, Q., et al. (2013b). Probing N^6-methyladenosine RNA modification status at single nucleotide resolution in mRNA and long noncoding RNA. RNA *19*, 1848–1856.

Liu, N., Zhou, K.I., Parisien, M., et al. (2017). N^6-methyladenosine alters RNA structure to regulate binding of a low-complexity protein. Nucleic Acids Res. *45*, 6051–6063.

Louloupi, A., Ntini, E., Conrad, T., et al. (2018). Transient N-6-methyladenosine transcriptome sequencing reveals a regulatory role of m^6A in splicing efficiency. Cell Rep. *23*, 3429–3437.

Luo, G.-Z., MacQueen, A., Zheng, G., et al. (2014). Unique features of the m^6A methylome in Arabidopsis thaliana. Nat. Commun. *5*, 5630.

Luo, S., and Tong, L. (2014). Molecular basis for the recognition of methylated adenines in RNA by the eukaryotic YTH domain. Proc. Natl Acad. Sci. USA *111*, 13834–13839.

Marondedze, C., Thomas, L., Serrano, N.L., et al. (2016). The RNA-binding protein repertoire of Arabidopsis thaliana. Sci. Rep. *6*, 29766.

Martinez, N.M., and Gilbert, W.V. (2018). Pre-mRNA modifications and their role in nuclear processing. Quant. Biol. *6*, 210–227.

Martinez-Perez, M., Aparicio, F., Lopez-Gresa, M.P., et al. (2017). Arabidopsis m^6A demethylase activity modulates viral infection of a plant virus and

the m^{6}A abundance in its genomic RNAs. Proc. Natl Acad. Sci. USA *114*, 10755–10760.

Mauer, J., Luo, X., Blanjoie, A., et al. (2017). Reversible methylation of m^{6}Am in the 5′ cap controls mRNA stability. Nature *541*, 371–375.

Meyer, K., Köster, T., Nolte, C., et al. (2017). Adaptation of iCLIP to plants determines the binding landscape of the clock-regulated RNA-binding protein AtGRP7. Genome Biol. *18*, 204.

Meyer, K.D., and Jaffrey, S.R. (2017). Rethinking m^{6}A readers, writers, and erasers. Annu. Rev. Cell Dev. Biol. *33*, 319–342.

Meyer, K.D., Patil, D.P., Zhou, J., et al. (2015). 5′ UTR m^{6}A promotes cap-independent translation. Cell *163*, 999–1010.

Meyer, K.D., Saletore, Y., Zumbo, P., et al. (2012). Comprehensive analysis of mRNA methylation reveals enrichment in 3′ UTRs and near stop codons. Cell *149*, 1635–1646.

Michlewski, G., and Caceres, J.F. (2019). Post-transcriptional control of miRNA biogenesis. RNA *25*, 1–16.

Mielecki, D., Zugaj, D.L., Muszewska, A., et al. (2012). Novel AlkB dioxygenases—alternative models for in silico and in vivo studies. PLoS One *7*, e30588.

Müller-McNicoll, M., Botti, V., de Jesus Domingues, A.M., et al. (2016). SR proteins are NXF1 adaptors that link alternative RNA processing to mRNA export. Genes Dev. *30*, 553–566.

Nichols, J.L. (1979). N^6-methyladenosine in maize poly(A)-containing RNA. Plant Sci. Lett. *15*, 357–361.

Ok, S.H., Jeong, H.J., Bae, J.M., et al. (2005). Novel CIPK1-associated proteins in Arabidopsis contain an evolutionarily conserved C-terminal region that mediates nuclear localization. Plant Physiol. *139*, 138–150.

Patil, D.P., Chen, C.K., Pickering, B.F., et al. (2016). m^{6}A RNA methylation promotes XIST-mediated transcriptional repression. Nature *537*, 369–373.

Pendleton, K.E., Chen, B., Liu, K., et al. (2017). The U6 snRNA m^{6}A methyltransferase METTL16 regulates SAM synthetase intron retention. Cell *169*, e814.

Perry, R.P., Kelley, D.E., Friderici, K., et al. (1975). The methylated constituents of L cell messenger RNA: evidence for an unusual cluster at the 5′ terminus. Cell *4*, 387–394.

Ping, X.L., Sun, B.F., Wang, L., et al. (2014). Mammalian WTAP is a regulatory subunit of the RNA N^6-methyladenosine methyltransferase. Cell Res. *24*, 177–189.

Reichel, M., Liao, Y., Rettel, M., et al. (2016). In planta determination of the mRNA-binding proteome of Arabidopsis etiolated seedlings. Plant Cell *28*, 2435–2452.

Ren, G., Xie, M., Dou, Y., et al. (2012). Regulation of miRNA abundance by RNA binding protein TOUGH in Arabidopsis. Proc. Natl Acad. Sci. USA *109*, 12817–12821.

Roost, C., Lynch, S.R., Batista, P.J., et al. (2015). Structure and thermodynamics of N^6-methyladenosine in RNA: a spring-loaded base modification. J. Am. Chem. Soc. *137*, 2107–2115.

Roundtree, I.A., Luo, G.Z., Zhang, Z., et al. (2017). YTHDC1 mediates nuclear export of N^6-methyladenosine methylated mRNAs. eLife *6*, e31311.

Ruzicka, K., Zhang, M., Campilho, A., et al. (2017). Identification of factors required for m^{6}A mRNA methylation in Arabidopsis reveals a role for the conserved E3 ubiquitin ligase HAKAI. New Phytol. *215*, 157–172.

Schöller, E., Weichmann, F., Treiber, T., et al. (2018). Interactions, localization, and phosphorylation of the m^{6}A generating METTL3–METTL14–WTAP complex. RNA *24*, 499–512.

Schwartz, S., Agarwala, S.D., Mumbach, M.R., et al. (2013). High-resolution mapping reveals a conserved, widespread, dynamic mRNA methylation program in yeast meiosis. Cell *155*, 1409–1421.

Schwartz, S., Mumbach, M.R., Jovanovic, M., et al. (2014). Perturbation of m^{6}A writers reveals two distinct classes of mRNA methylation at internal and 5′ sites. Cell Rep. *8*, 284–296.

Scutenaire, J., Deragon, J.-M., Jean, V., et al. (2018). The YTH domain protein ECT2 is an m^{6}A reader required for normal trichome branching in Arabidopsis. Plant Cell *30*, 986–1005.

Shen, L., Liang, Z., Gu, X., et al. (2016). N^6-Methyladenosine RNA modification regulates shoot stem cell fate in Arabidopsis. Dev. Cell *38*, 186–200.

Shi, H., Wang, X., Lu, Z., et al. (2017). YTHDF3 facilitates translation and decay of N^6-methyladenosine-modified RNA. Cell Res. *27*, 315–328.

Slobodin, B., Han, R., Calderone, V., et al. (2017). Transcription impacts the efficiency of mRNA translation via co-transcriptional N^6-adenosine methylation. Cell *169*, 326–337.e12.

Squires, J.E., Patel, H.R., Nousch, M., et al. (2012). Widespread occurrence of 5-methylcytosine in human coding and non-coding RNA. Nucleic Acids Res. *40*, 5023–5033.

Srikanth, A., and Schmid, M. (2011). Regulation of flowering time: all roads lead to Rome. Cell. Mol. Life Sci. *68*, 2013–2037.

Tang, C., Klukovich, R., Peng, H., et al. (2018). ALKBH5-dependent m^{6}A demethylation controls splicing and stability of long 3′-UTR mRNAs in male germ cells. Proc. Natl Acad. Sci. USA *115*, E325–E333.

Theler, D., Dominguez, C., Blatter, M., et al. (2014). Solution structure of the YTH domain in complex with N^6-methyladenosine RNA: a reader of methylated RNA. Nucleic Acids Res. *42*, 13911–13919.

Thomas, P.E., Wu, X., Liu, M., et al. (2012). Genome-wide control of polyadenylation site choice by CPSF30 in Arabidopsis. Plant Cell *24*, 4376–4388.

Ule, J., Jensen, K.B., Ruggiu, M., et al. (2003). CLIP identifies Nova-regulated RNA networks in the brain. Science *302*, 1212–1215.

Uranishi, H., Zolotukhin, A.S., Lindtner, S., et al. (2009). The RNA-binding motif protein 15B (RBM15B/OTT3) acts as cofactor of the nuclear export receptor NXF1. J. Biol. Chem. *284*, 26106–26116.

Vespa, L., Vachon, G., Berger, F., et al. (2004). The Immunophilin-interacting protein AtFIP37 from Arabidopsis is essential for plant development and is involved in trichome endoreduplication. Plant Physiol. *134*, 1283–1292.

Wan, Y., Tang, K., Zhang, D., et al. (2015). Transcriptome-wide high-throughput deep m^{6}A-seq reveals unique differential m^{6}A methylation patterns between three organs in Arabidopsis thaliana. Genome Biol. *16*, 272.

Wang, X., Feng, J., Xue, Y., et al. (2016). Structural basis of N^6-adenosine methylation by the METTL3–METTL14 complex. Nature *534*, 575–578.

Wang, X., Lu, Z., Gomez, A., et al. (2014a). N^6-methyladenosine-dependent regulation of messenger RNA stability. Nature *505*, 117–120.

Wang, X., Zhao, B.S., Roundtree, I.A., et al. (2015). N^6-methyladenosine modulates messenger RNA translation efficiency. Cell *161*, 1388–1399.

Wang, Y., Li, Y., Toth, J.I., et al. (2014b). N^6-methyladenosine modification destabilizes developmental regulators in embryonic stem cells. Nat. Cell Biol. *16*, 191–198.

Warda, A.S., Kretschmer, J., Hackert, P., et al. (2017). Human METTL16 is a N^6-methyladenosine (m^{6}A) methyltransferase that targets pre-mRNAs and various non-coding RNAs. EMBO Rep. *18*, 2004–2014.

Wei, C.M., and Moss, B. (1977). Nucleotide sequences at the N^6-methyladenosine sites of HeLa cell messenger ribonucleic acid. Biochemistry *16*, 1672–1676.

Wei, L.-H., Song, P., Wang, Y., et al. (2018). The m^{6}A reader ECT2 controls trichome morphology by affecting mRNA stability in Arabidopsis. Plant Cell *30*, 968–985.

Wojtas, M.N., Pandey, R.R., Mendel, M., et al. (2017). Regulation of m^{6}A transcripts by the 3′→5′ RNA helicase YTHDC2 is essential for a successful meiotic program in the mammalian germline. Mol. Cell *68*, 374–387.e12.

Wu, R., Li, A., Sun, B., et al. (2019). A novel m^{6}A reader Prrc2a controls oligodendroglial specification and myelination. Cell Res. *29*, 23–41.

Xiao, W., Adhikari, S., Dahal, U., et al. (2016). Nuclear m^{6}A reader YTHDC1 regulates mRNA splicing. Mol. Cell *61*, 507–519.

Xu, C., Wang, X., Liu, K., et al. (2014). Structural basis for selective binding of m^{6}A RNA by the YTHDC1 YTH domain. Nat. Chem. Biol. *10*, 927–929.

Yu, J., Chen, M., Huang, H., et al. (2018). Dynamic m^{6}A modification regulates local translation of mRNA in axons. Nucleic Acids Res. *46*, 1412–1423.

Yue, Y., Liu, J., Cui, X., et al. (2018). VIRMA mediates preferential m^{6}A mRNA methylation in 3′UTR and near stop codon and associates with alternative polyadenylation. Cell Discov. *4*, 10.

Zhang, J., Addepalli, B., Yun, K.Y., et al. (2008). A polyadenylation factor subunit implicated in regulating oxidative signaling in Arabidopsis thaliana. PLoS One *3*, e2410.

Zhang, Y., Gu, L., Hou, Y., et al. (2015). Integrative genome-wide analysis reveals HLP1, a novel RNA-binding protein, regulates plant flowering by targeting alternative polyadenylation. Cell Res. *25*, 864–876.

Zhang, Z., Boonen, K., Ferrari, P., et al. (2016). UV crosslinked mRNA-binding proteins captured from leaf mesophyll protoplasts. Plant Methods *12*, 42.

Zheng, G., Dahl, J.A., Niu, Y., et al. (2013). ALKBH5 is a mammalian RNA demethylase that impacts RNA metabolism and mouse fertility. Mol. Cell *49*, 18–29.

Zhong, S., Li, H., Bodi, Z., et al. (2008). MTA is an Arabidopsis messenger RNA adenosine methylase and interacts with a homolog of a sex-specific splicing factor. Plant Cell *20*, 1278–1288.

Zhou, J., Wan, J., Gao, X., et al. (2015). Dynamic m^6A mRNA methylation directs translational control of heat shock response. Nature *526*, 591–594.

Zhu, T., Roundtree, I.A., Wang, P., et al. (2014). Crystal structure of the YTH domain of YTHDF2 reveals mechanism for recognition of N^6-methyladenosine. Cell Res. *24*, 1493–1496.

Zolotukhin, A.S., Uranishi, H., Lindtner, S., et al. (2009). Nuclear export factor RBM15 facilitates the access of DBP5 to mRNA. Nucleic Acids Res. *37*, 7151–7162.